JAUES

Journal of Al Azhar University Engineering Sector

Vol. 7, No. 24, July 2012, 1531-1544

GLOBALLY STABLE INTEGRATED KINEMATIC AND DYNAMIC CONTROL FOR TRAJECTORY TRACKING OF A MOBILE ROBOT PROVIDED WITH CASTER WHEEL

Ayman A. El-Badawy[1] and Amr Y. Mowafy[2]

[1]Mechanical Engineering Dept. Faculty of Engineering, AL-Azhar University, Cairo, Egypt,

[2]Tecnomare S.P.A-Eni for offshore and Subsea Projects engineering

ABSTRACT

In this paper, a non-linear control law, for nonholonomic mobile robots, that integrates kinematic controller with dynamic controller is presented in order to track a reference trajectory. The global asymptotic stability of the control law is proven using Lyapunov theory. The global stability is guaranteed since all the error states (position, orientation, linear and angular velocities) are presented in both the Lyapunov function and its derivative. The control law is implemented on a dynamic model of a differential-drive mobile robot that takes into consideration caster wheel effect. The generalized force created by the caster wheel is implemented using the virtual displacement method. Numerical simulations supported by experimental verification show that the integrated globally stable developed control law provides faster convergence to the reference path and eliminates overshoot over the kinematic controller alone.

KEYWORDS: Trajectory-Tracking, Lyapunov, Asymptotic Stability, Caster Wheel, Mobile Robot

1. INTRODUCTION

Autonomous vehicles are used in space explorations, mine removal, factories, hospitals, rescue activities in catastrophic events, military service and even in museums and commercial public places where they become a source of attraction to visitors and clients [1]. Many researchers investigate various tracking control methods considering the non-holonomic constraints of mobile robots. Kanayama et al. proposed a path tracking control rule to find a reasonable target linear and rotational velocities. In their work, perfect velocity tracking was assumed which simplified their analysis [2]. Fierro and Lewis made a dynamical extension that made possible the integration of a kinematic controller and a torque controller for nonholonomic mobile robots. Their result is a general structure that can accommodate different control techniques, ranging from a computed-torque controller to robust-adaptive controller based on neural networks [3]. Guo et al. proposed a method of global trajectory generation that is composed of regional path segments, which are parametric polynomials incorporating collision avoidance criteria [4]**.** Bakker et al. proposed a path following control that minimizes the orthogonal distance and orientation error to the desired path of a platform that is four-wheel steered and four-wheel driven [5]. Lee et al. proposed a method to plan a path and control the position of wheeled mobile robot (WMR) in a robot soccer

game. To tackle the difficulties of the nonlinear control problem, the motion of the WMR is realized via changing the linear displacement and angular displacement in a separate manner such that the WMR is either rotating or moving in a straight line at any one time [6]. Oh et al. proposed a wavelet based fuzzy neural network (WFNN) based direct adaptive control scheme for the solution of the tracking problem of mobile robots. In addition, an approach that uses adaptive learning rates for training of the WFNN controller is driven via a Lyapunov stability analysis to guarantee fast convergence [7]. Martinez et al. proposed a path tracking technique for non-holonomic mobile robots tractors with a trailer. The main advantage of their pure geometric technique is that no kinematic model of the vehicle was needed [8].

Most of the developed controllers consider only the kinematic model of the mobile robot, there are several problems with this approach; first, the perfect velocity tracking assumption does not hold in practice; second, disturbances are ignored. Thus, to improve the performance of any newly developed controller, a better knowledge of the robot dynamics is required. Chen and Dao developed equations of motion describing the motions of a bicycle using Lagrange's equations for quasi-coordinates. Based on the developed equations of motion and by considering the distance from the reference point to the target path and the heading direction of the bicycle, control schemes based on fuzzy and proportional-integral-derivative (PID) controllers have been proposed and discussed [9]. F. Han described a new type of nonholonomic and omni-directional mobile robot using two driving assemblies, one of which consists of two independent driving wheel mechanisms. They derived kinematic models of a wheel mechanism and of a mobile robot with two driving assemblies, where these models are applied to construct a feedback control system for the robot [10]. S. Staicu analyzed the kinematics and dynamics of a mobile robot, consisting of a platform, two conventional wheels and a crank that controls the motion of a free rolling caster wheel. Based on several matrix relations of connectivity, he derived the characteristic velocities and accelerations of this nonholonomic mechanical system [11].

In this paper, a non-linear control law that integrates kinematic and dynamic controllers in one algorithm is presented. The kinematic control is responsible to minimize the position and orientation errors of the mobile robot with respect to the reference path. The dynamic control is responsible to minimize the difference between the reference velocities and the actual velocities which are computed from the dynamic model in case of simulation or extracted from sensors in case of experimental work. This type of control algorithm requires a complete knowledge of the dynamics of the non-holonomic robot that will be controlled. Hence, the caster wheel effect for a differential-drive robot is taken into consideration. The caster wheel affects the robot chassis through forces acting at the caster assembly pivot. The global asymptotic stability of the control law is proven using Lyapunov direct method. The global stability is guaranteed based on the presence of all the state errors in the developed Lyapunov function and in its derivative. The dynamic control provides faster convergence to the reference path and eliminates overshoot in robot motion than just pure kinematic control. Experimental verification was implemented on a differentially-driven robot to test the performance of the proposed controller.

2. DYNAMIC MODEL OF A DIFFERENTIAL-DRIVE ROBOT PROVIDED WITH CASTER WHEEL

The differential-drive autonomous vehicle shown in Figure 1 is a typical example of a nonholonomic mobile robot. It consists of a vehicle with two driving wheels mounted on the same axis, and a front caster wheel. The motion and orientation are achieved by independent actuators, e.g. DC motors, providing the necessary torques to the rear wheels.

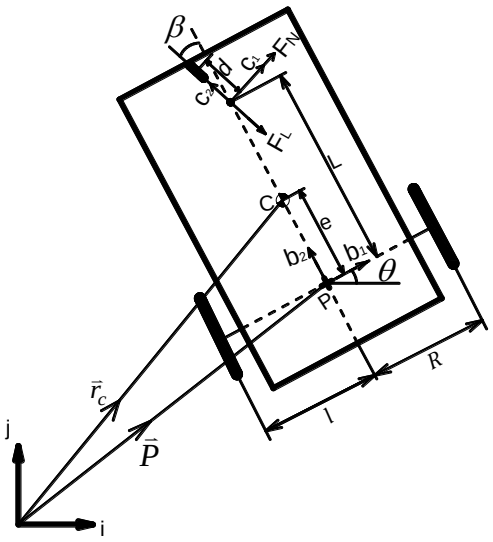

Fig. 1. Differential-Drive Robot

Using a global coordinate system, the position of the vehicle turning center, as a function of time, can be specified as a vector quantity

$$\vec{\mathbf{P}}(t) = x(t)\hat{\mathrm{i}} + y(t)\hat{\mathrm{j}}$$

where $x(t)$ is the position along the x-axis and $y(t)$ is the position along the y-axis, both as a function of time, and $\hat{\mathrm{i}}$ and $\hat{\mathrm{j}}$ are unit vectors along the fixed x- and y-axes, respectively. The vector pointing to the center of mass (*C*) can be calculated as

$$\vec{\mathbf{r}}_c = \vec{\mathbf{P}} - e\,\hat{\mathrm{b}}_2$$

where $\hat{\mathrm{b}}_1, \hat{\mathrm{b}}_2, \hat{\mathrm{b}}_3$ represent unit vectors in the body coordinate frame, and *e* is the distance from the center of rotation to the center of mass. The kinematics of a differential-drive mobile robot described in the global reference frame is given by

$$\begin{bmatrix} \dot{x} \\ \dot{y} \\ \dot{\theta} \end{bmatrix} = \begin{bmatrix} \cos\theta & 0 \\ \sin\theta & 0 \\ 0 & 1 \end{bmatrix} \begin{bmatrix} v \\ \omega \end{bmatrix} \tag{1}$$

where $\dot{x}$, $\dot{y}$ and $\dot{\theta}$ are the linear and angular velocities in the global reference frame, and *v* and ω are the vehicle speed and turning rate respectively.

The speed of the vehicle *v*, along the path traveled by the turning center, is given by a weighted average of the speeds of the two driving wheels. Also, the rate of change of heading, or turning rate ω, can be computed as the vehicle is rotating about an instant center. Combining these relations yields a kinematic model for the differential-drive robot

$$\begin{bmatrix} v \\ \omega \end{bmatrix} = \frac{1}{l+R} \begin{bmatrix} R r_{wr} & l r_{wl} \\ r_{wr} & -r_{wl} \end{bmatrix} \begin{bmatrix} \dot{\varphi}_r \\ \dot{\varphi}_l \end{bmatrix} \tag{2}$$

where l, R are the distances from the centerline of the robot chassis to the left and right wheel respectively. r_{wr}, r_{wl} are the radii of the right and left driving wheels of the robot, and $\dot{\varphi}_r$, $\dot{\varphi}_l$ are the spinning velocities of the right and left wheels. In this work, flat plane motion is assumed, wheels roll without slipping, bearing friction follows a simple viscous model with C_l and C_r are the viscous damping coefficients for the left and right wheels respectively. Finally the caster effects on the vehicle are modeled using forces acting on the caster pivot.

The Lagrange formalism is used to find the dynamic equations of the mobile robot. Because the trajectory of the mobile base is constrained to the horizontal plane, its potential energy remains constant. The kinetic energy which is decomposed into that of the main vehicle body and that of the two drive wheels is given by

$$T = \frac{1}{2} m_R \left(\frac{l r_{wl} \dot{\varphi}_l + R r_{wr} \dot{\varphi}_r}{l + R} \right)^2 + \frac{1}{2} I_R \left(\frac{r_{wr} \dot{\varphi}_l - r_{wl} \dot{\varphi}_l}{l + R} \right)^2 + \frac{1}{2} I_l \dot{\varphi}_l^2 + \frac{1}{2} I_r \dot{\varphi}_r^2 \qquad (3)$$

where m_R is the robot mass, I_R is the mass moment of inertia of the robot about the center of rotation and I_l and I_r are the mass moments of inertia of the left and right wheels respectively . Also, the total kinetic energy of the caster assembly is being neglected. However, the mass of the caster wheel is lumped with the mass of the vehicle, then only the rotational energy of the caster is neglected.

The caster wheel affects the robot chassis through forces which are decomposed into two component forces as shown in figure (1). One component acts along the direction that the caster wheel is rolling ($\mathbf{F}_L$). This component is a drag force which is due to rolling friction force encountered by the caster wheel. The other force is assumed to be perpendicular to the caster path ($\mathbf{F}_N$). This force enforces the no-slide-slip constraint on the caster wheel. All these three types of external forces will be treated as generalized forces. The generalized force created from the caster wheel forces can be expressed by

$$Q_j = \vec{F}_L \bullet \frac{\partial \vec{D}}{\partial q_j} + \vec{F}_N \bullet \frac{\partial \vec{D}}{\partial q_j} \qquad (4)$$

where $\partial \vec{D}$ is the virtual displacement of the caster wheel pivot. The virtual displacement is supposed to be due to the movement of the center of rotation midpoint P adding to it the movement of the pivot relative to the center of rotation midpoint P for a virtual displacement of the generalized coordinates. In the local reference frame, the virtual displacement is given by

$$\delta \vec{D} = \left\{ \frac{l r_{wl} \delta\varphi_l + R r_{wr} \delta\varphi_r}{l + R} \right\} \hat{b}_2 - L \left\{ \frac{r_{wr} \delta\varphi_r - r_{wl} \delta\varphi_l}{l + R} \right\} \hat{b}_1 \qquad (5)$$

The two longitudinal and normal forces of the caster wheel are expressed in the caster wheel coordinates and so it must be converted to the local reference frame coordinates. The caster wheel coordinate frame is rotated with respect to the body coordinate frame by the negative of the caster wheel angle β. The caster coordinates can be expressed in the body coordinate frame as

$$\hat{c}_1 = \cos\beta\,\hat{b}_1 + \sin\beta\,\hat{b}_2$$
$$\hat{c}_2 = -\sin\beta\,\hat{b}_1 + \cos\beta\,\hat{b}_2 \quad (6)$$

hence, the caster wheel forces in the local reference frame are

$$\vec{F}_L = -F_L\left(-\sin\beta\,\hat{b}_1 + \cos\beta\,\hat{b}_2\right) \quad (7)$$
$$\vec{F}_N = F_N\left(\cos\beta\,\hat{b}_2 + \sin\beta\,\hat{b}_2\right) \quad (8)$$

using equations (5), (7) and (8) in equation (4), the total generalized force including the driving torque and the rolling friction on the right and left driving wheels are:

$$\begin{aligned}\left(Q_{Tot}\right)_r &= k_{tr} i_{ar} - C_f\, N_r\, r_r - \frac{r_{wl}\left(F_N \sin\beta - F_L \cos\beta\right)l - L\left(F_N \cos\beta + F_L \sin\beta\right)r_{wl}}{R+l} \\ \left(Q_{Tot}\right)_l &= k_{tl} i_{al} - C_f\, N_l\, r_l - \frac{L\left(F_N \cos\beta + F_L \sin\beta\right)r_{wl} + r_{wl}\left(F_N \sin\beta - F_L \cos\beta\right)l}{R+l}\end{aligned} \quad (9)$$

where for a DC motor, the motor torque transferred to each wheel is the given by the product of K_t (the motor torque constant), and i_a (the armature current). The rolling friction force ($\mathbf{F}_L$) between the wheels and the ground is proportional to the force (**N**) due to the weight of the robot acting on a contact point with C_f being the proportionality constant. Choosing a state vector $\vec{\mathbf{X}} = \left[\varphi_l \quad \varphi_r \quad \dot{\varphi}_l \quad \dot{\varphi}_r\right]^T$, and input vector as $\vec{\mathbf{U}} = \left[i_{al} \quad i_{ar} \quad C_{fl} \quad C_{fr} \quad F_N \quad F_L\right]^T$, the following state space model of the differential-drive robot can be developed:

$$\begin{bmatrix}\dot{\varphi}_l \\ \dot{\varphi}_r \\ \ddot{\varphi}_l \\ \ddot{\varphi}_r\end{bmatrix} = \begin{bmatrix}0 & 0 & 1 & 0 \\ 0 & 0 & 0 & 1 \\ 0 & 0 & A_{33} & A_{34} \\ 0 & 0 & A_{43} & A_{44}\end{bmatrix}\begin{bmatrix}\varphi_l \\ \varphi_r \\ \dot{\varphi}_l \\ \dot{\varphi}_r\end{bmatrix} + \begin{bmatrix}0 & 0 & 0 & 0 & 0 & 0 \\ 0 & 0 & 0 & 0 & 0 & 0 \\ B_{31} & B_{32} & B_{33} & B_{34} & B_{35} & B_{36} \\ B_{41} & B_{42} & B_{43} & B_{44} & B_{45} & B_{46}\end{bmatrix}\begin{bmatrix}i_{al} \\ i_{ar} \\ C_{fl} \\ C_{fr} \\ F_N \\ F_L\end{bmatrix} \quad (10)$$

where A_{ij}, B_{ij} coefficients are defined in appendix A. In this model, the caster effect is treated as external forces that remain as unknowns and thus need to be determined.

Figure (2) shows the caster assembly as a free-body diagram with the forces and moments shown. F_N and F_L are the reaction forces at the caster pivot, equal and opposite to the forces on the vehicle. F_{NG} and F_{LG} are the ground contact forces, where F_{NG} is the constraint force which prevents side-slip and F_{LG} is the drag force due to the rolling friction on the caster wheel. This drag force is assumed proportional to the weight on the caster wheel, given by

$$F_{NG} = C_{fc} N_c \quad (11)$$

where C_{fc}, N_c are the coefficient of rolling friction at the caster wheel, and the weight on the caster wheel respectively.

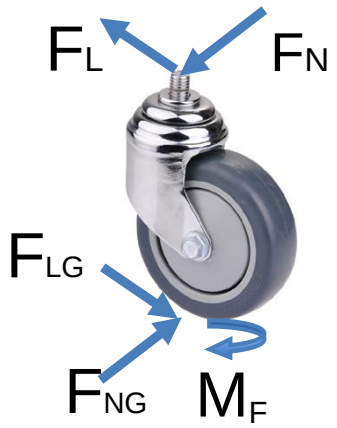

Fig. (2) Caster Wheel Free Body Diagram

The moment, M_F, represents the combination of ground friction and pivot friction that opposes the caster wheel rotation. This relationship is given by

$$M_F = \mathrm{k}_F \operatorname{sgn}(\dot{\beta}) \tag{12}$$

where k_F is constant moment and $\operatorname{sgn}(\dot{\beta})$ is the signum function, ±1 or 0 depending upon direction of caster assembly rotation. In this development, the moment is positive in a right hand sense, while the caster angle is positive in a left hand sense. Therefore, the constant k_F is positive.

Assuming negligible mass and inertia of the caster wheel assembly consistent with the previous assumptions, the reaction forces are given by

$$F_N = F_{NG} = -\frac{\mathrm{k}_F}{d}\operatorname{sgn}(\dot{\beta}) \tag{13}$$

$$F_L = C_{fc} N_c \tag{14}$$

where *d* is the projected planar distance between caster pivot and ground contact. This leaves only the rate of rotation of caster wheel, $\dot{\beta}$, to be calculated. The velocity of the caster pivot, in vehicle body coordinates, is given by

$$\vec{V}_c = v\hat{\mathrm{b}}_2 + \dot{\theta}\hat{\mathrm{b}}_3 \times \left(L\hat{\mathrm{b}}_2\right) = v\hat{\mathrm{b}}_2 - L\dot{\theta}\hat{\mathrm{b}}_1,$$

which can be converted to caster assembly coordinates as

$$\vec{V}_c = \left\{v\sin(\beta) - L\dot{\theta}\cos\beta\right\}\hat{\mathrm{c}}_1 + \left\{v\cos(\beta) + L\dot{\theta}\sin\beta\right\}\hat{\mathrm{c}}_2$$

The velocity of the point of ground contact on the caster wheel is given by

$$\vec{V}_{Gc} = \vec{V}_c - \dot{\beta}\hat{\mathrm{c}}_3 \times \left(-d\,\hat{\mathrm{c}}_2\right)$$

or it can be written as

$$\vec{V}_c = \left\{v\sin(\beta) - L\dot{\theta}\cos\beta - \dot{\beta}d\right\}\hat{\mathrm{c}}_1 + \left\{v\cos(\beta) + L\dot{\theta}\sin\beta\right\}\hat{\mathrm{c}}_2$$

However, the no-slide-slip constraint requires that the $\hat{\mathrm{c}}_1$ component of velocity equal zero, therefore

$$\dot{\beta} = \frac{\left(v\sin(\beta) - L\dot{\theta}\cos(\beta)\right)}{d} \tag{15}$$

By substituting equation (2) in (15) the rate of caster wheel rotation is:

$$\dot{\beta} = \frac{\{l\sin(\beta) + L\cos(\beta)\}r_{wl}\dot{\varphi}_l + \{R\sin(\beta) - L\cos(\beta)\}r_{wr}\dot{\varphi}_r}{d\,(l+R)} \tag{16}$$

In order to obtain the steering angle, β, the rate of rotation $\dot{\beta}$ can be numerically integrated. The calculation of the final three unknowns $\dot{\beta}$, F_L, and F_N completes the dynamic modeling and allows the effects of the caster assembly to be included in the nonlinear dynamic model. The comparison of actual data to the numerical simulations of the analytical model provides the basis for accepting or rejecting the assumptions put forth during the development of the model.

3. INTEGRATED CONTROLLER DESIGN METHODOLOGY

3.1 Control Law Development

In this section, a globally asymptotically stable control law tracking a reference trajectory is presented. The global input of the system is the reference configuration $\mathbf{B_G} = [x_G, y_G, \theta_G]^T$ and reference velocities $\mathbf{u}_G = [v_G \quad \omega_G]^T$ which are both of variables of time. The global output of the system is the actual current configuration $\mathbf{B_A} = [x_A, y_A, \theta_A]^T$. The purpose of the tracking controller is to converge the error configuration $\mathbf{B}_e = [e_1, e_2, e_\theta]^T$ to zero.

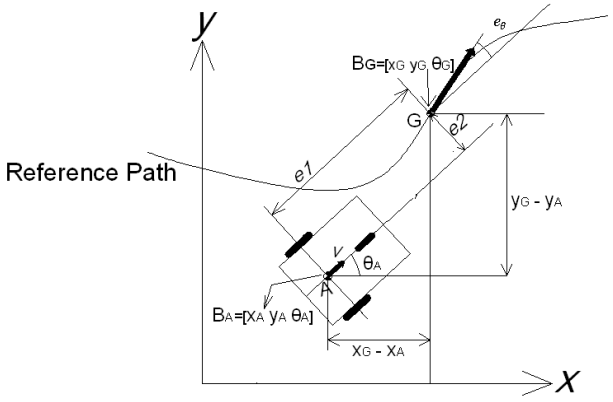

Fig. 3. Concept Of Error Posture

Figure 3 represents the concept of the error posture $\mathbf{B}_e = [e_1, e_2, e_\theta]^T$ which is a transformation of the reference posture, $\mathbf{B_G}$ in a local coordinate system with an origin of (x_A, y_A) and an x-axis in the direction of θ_A and is given by

$$\mathbf{B}_e = \begin{bmatrix} e_1 \\ e_2 \\ e_\theta \end{bmatrix} = \mathbf{T_e}(\mathbf{B_G} - \mathbf{B_A}) = \begin{bmatrix} \cos\theta_A & \sin\theta_A & 0 \\ -\sin\theta_A & \cos\theta_A & 0 \\ 0 & 0 & 1 \end{bmatrix} \begin{bmatrix} x_G - x_A \\ y_G - y_A \\ \theta_G - \theta_A \end{bmatrix} \tag{17}$$

and the derivative of the error is

$$\dot{\mathbf{B}}_{\mathbf{e}} = f(t,\mathbf{B}_{\mathbf{e}}) = \begin{bmatrix} \dot{e}_1 \\ \dot{e}_2 \\ \dot{e}_\theta \end{bmatrix} = \begin{bmatrix} e_2\omega_A - v_A + v_G \cos e_\theta \\ -e_1\omega_A + v_G \sin e_\theta \\ \omega_G - \omega_A \end{bmatrix} \tag{18}$$

where $\mathbf{q}_A = [v_A \quad \omega_A]^T$ are the actual linear and angular velocities computed from the dynamic model in case of simulation, equations (2) and (10), or obtained from the sensor measurements in case of experimental work. Equation (18) demonstrates that $\dot{\mathbf{B}}_e$ is a function of $\mathbf{B}_e$, $\mathbf{B}_G$, $\mathbf{u}_G$ and $\mathbf{q}_A$. Since $\mathbf{B}_G$ and $\mathbf{u}_G$ are functions of time *t* and $\mathbf{B}_e$. A nonlinear path tracking controller is proposed for the target velocities as follows:

$$\mathbf{q}_{\mathrm{k}} = \begin{bmatrix} v_{\mathrm{k}} \\ \omega_{\mathrm{k}} \end{bmatrix} = \begin{bmatrix} v_{\mathrm{k}}(\mathbf{B}_{\mathrm{e}},\mathbf{u}_{\mathrm{G}}) \\ \omega_{\mathrm{k}}(\mathbf{B}_{\mathrm{e}},\mathbf{u}_{\mathrm{G}}) \end{bmatrix} = \begin{bmatrix} v_{\mathrm{G}} \cos e_\theta + k_1 e_1 - k_\theta e_\theta \omega_k \\ \omega_{\mathrm{G}} + v_{\mathrm{G}} k_2 (e_2 + k_\theta e_\theta) + \dfrac{v_{\mathrm{G}}}{k_\theta} \sin e_\theta \end{bmatrix} \tag{19}$$

where k_1, k_2, and k_θ are positive constant parameters. $v_{\mathrm{G}} \cos e_\theta$ and ω_{G} are feedforward terms that are used to eliminate steady-state error. Hence, The derivative of the velocity inputs would be proportional to torque input to the motors and is given by

$$\dot{\mathbf{q}}_{\mathrm{k}} = \begin{bmatrix} \dot{v}_{\mathrm{k}} \\ \dot{\omega}_{\mathrm{k}} \end{bmatrix} = \begin{bmatrix} v_{\mathrm{k}}(\mathbf{B}_{\mathrm{e}}(t),\mathbf{u}_{\mathrm{G}}) \\ \omega_{\mathrm{k}}(\mathbf{B}_{\mathrm{e}}(t),\mathbf{u}_{\mathrm{G}}) \end{bmatrix} = \begin{bmatrix} -v_{\mathrm{G}} \dot{e}_\theta \sin e_\theta + k_1 \dot{e}_1 - k_\theta \dot{e}_\theta \omega - k_\theta e_\theta \dot{\omega} \\ v_{\mathrm{G}} k_2 (e_2 + k_\theta e_\theta)(\dot{e}_2 + k_\theta \dot{e}_\theta) + \dfrac{v_{\mathrm{G}}}{k_\theta} \dot{e}_\theta \cos e_\theta \end{bmatrix} \tag{20}$$

The kinematic controller represented by equation (20) follows the perfect velocity tracking assumption. The perfect velocity tracking assumption stands for the idea that the mobile robot hardware is capable of transforming target velocities to real current velocities and thus neglecting dynamics effect. In fact, implementing such control law can be enhanced by including a velocity tracking inner loop that represents the deviation between actual velocities determined from dynamic model, or from experimental measurements, and the required velocities determined from the kinematic model (equation 19). Hence, an integrated nonlinear control law of the following form can be employed

$$\mathbf{u} = \dot{\mathbf{q}}_{\mathrm{k}} + \dot{\mathbf{q}}_{\mathrm{d}} \tag{21}$$

where $\dot{\mathbf{q}}_{\mathrm{d}} = -\mathbf{K}_d(\mathbf{q}_A - \mathbf{q}_K)$ and $\mathbf{k}_d$ is a positive definite diagonal matrix given by $\mathbf{k}_d = k_d\mathbf{I}$. Lets define $\mathbf{e}_d = \mathbf{q}_A - \mathbf{q}_k$ therefore $\dot{\mathbf{q}}_{\mathrm{d}} = -\mathbf{K}_d\mathbf{e}_d$.

3.2 Stability Analysis

In this section, the global asymptotic stability of the developed control law is proved using Lyapunov direct method. The global stability is guaranteed based on the presence of all the state errors including orientation and velocity errors in the proposed Lyapunov function and its derivative. Consider the following Lyapunov function candidate:

$$V = k_1 e_1^{\,2} + k_1(e_2 + k_\theta e_\theta)^2 + \frac{2k_1}{k_2}(1 - \cos e_\theta) + \frac{1}{2k_d} e_3^2 + \frac{k_1 k_\theta}{2k_d k_2 v_G} e_4^2 \tag{22}$$

Definitely, $V > 0$ at $\mathbf{B_e} \neq 0$ and $V(x) = 0$ at $\mathbf{B_e} = 0$, consequently V is positive definite. The time derivative of V is

$$\dot{V} = 2k_1 e_1 \dot{e}_1 + 2k_2 (e_2 + k_\theta e_\theta)(\dot{e}_2 + k_\theta \dot{e}_\theta) + \frac{2k_1}{k_2} \dot{e}_\theta \sin e_\theta - e_3^2 - \frac{k_1 k_\theta}{k_2 v_G} e_4^2$$

$$\dot{V} = 2k_1 e_1 (e_2 \omega_A - v_A + v_G \cos e_\theta) + 2k_1 (e_2 + k_\theta e_\theta)\dot{e}_2 + (e_2 + k_\theta e_\theta) k_\theta \dot{e}_\theta + \frac{2k_1}{k_2} (\sin e_\theta)(\omega_G - \omega_A)$$

$$- (v_A - k_1 e_1 - v_G \cos e_\theta + k_\theta e_\theta \omega_k)^2 - \frac{k_1 k_\theta}{k_2 v_G} \left(\omega_A - \omega_G - k_2 v_G (e_2 + k_\theta e_\theta) - \frac{v_G}{k_\theta} \sin e_\theta \right)^2$$

$$\dot{V} = -(e_1 + k_1 e_1)^2 - k_2^2 v_G^2 (e_2 + k_\theta e_\theta)^2 - \frac{2k_1 v_G^2}{k_\theta^2} \sin^2 e_\theta - \frac{k_1 k_\theta}{k_2 v_G} \left\{ e_4 + k_2 (e_2 + k_\theta e_\theta)^2 + \frac{v_G}{k_\theta} \sin e_\theta \right\}^2$$

$\dot{V}$ is negative definite, since $\dot{V} < 0$ at $\mathbf{B_e} \neq 0$ and $\dot{V} = 0$ at $\mathbf{B_e} = 0$. Since $\dot{V}$ contains all of the error states, therefore the equilibrium point $\mathbf{B_e} = 0$ is globally asymptotically stable.

Figure 4 shows the general architecture for the developed globally asymptotically stable tracking control system.

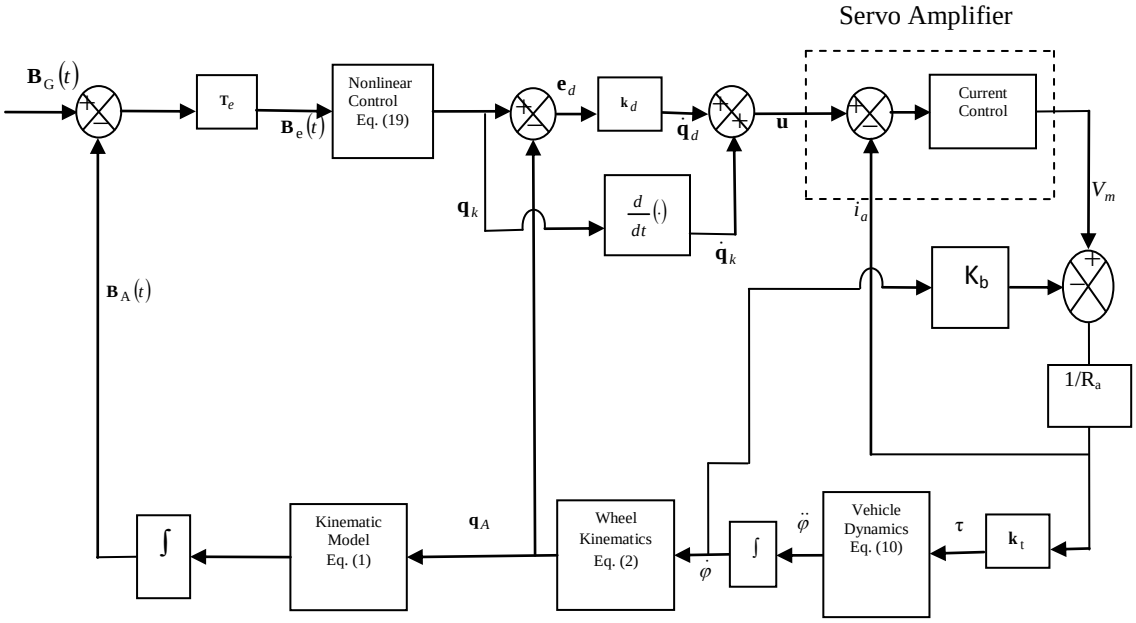

Figure 4 Control System Architecture

Here V_m is the motor control voltage, R_a and K_b are the armature resistance and back emf for a DC motor respectively.

3.3 Determining Control Parameters

Although the stability of the control system is guaranteed for any combination of the positive constants k_1, k_2, k_θ, a non-oscillatory, but not too slow response of the robot is required, so an optimal solution must be implemented. In order to tune the control parameters of the kinematic controller, the system is linearized around the equilibrium point $\mathbf{B}_e = 0$. The constant matrix of the linearized system, after substitution of equation (19) in (18), is given by

$$A = \left(\frac{\partial f(t, \mathbf{B_e})}{\partial \mathbf{B_e}} \right)_{\mathbf{B_e}=0} \tag{23}$$

By applying equation (23) the A matrix is given by

$$A = \begin{bmatrix} -k_1 & \omega_G & k_\theta \omega_G \\ -\omega_G & 0 & v_G \\ 0 & -v_G k_2 & -v_G\left(k_2 k_\theta + \dfrac{1}{k_\theta}\right) \end{bmatrix},$$

where A is bounded and continuously differentiable constant matrix.

For simplification of the analysis, the situation in which the reference configuration is moving on the x-axis to the positive direction at a constant velocity v_G is considered. Mathematically this condition can be written as follows:

$$\mathbf{B_G} = \begin{bmatrix} x_G(t) \\ y_G(t) \\ \theta_G(t) \end{bmatrix} = \begin{bmatrix} v_G t \\ 0 \\ 0 \end{bmatrix} \tag{24}$$

$$\mathbf{u_G} = \begin{bmatrix} v_G \\ \omega_G \end{bmatrix} = \begin{bmatrix} v_G \\ 0 \end{bmatrix} \tag{25}$$

This condition is called the linear reference motion. In addition we assume that,

$$|\theta_e| << 1 \qquad \text{and} \quad |\dot{\theta}_e| << 1 \tag{26}$$

From (17) and (23),

$$\dot{\mathbf{T}}_e(\mathbf{B}_G - \mathbf{B}_A) + \mathbf{T}_e(\dot{\mathbf{B}}_G - \dot{\mathbf{B}}_A) = \mathbf{A}\mathbf{T}_\mathbf{e}(\mathbf{B}_G - \mathbf{B}_A)$$

$$\dot{\mathbf{B}}_A = \mathbf{T}_e^{-1}(\mathbf{A}\mathbf{T}_e - \dot{\mathbf{T}}_e)(\mathbf{B}_G - \mathbf{B}_A) + \dot{\mathbf{B}}_G \tag{27}$$

Condition (24) indicates that θ_G =0.Therefore

$$|\theta_A| = |\theta_e| << 1 \qquad \text{and} \qquad |\dot{\theta}_A| = |\dot{\theta}_e| << 1 \tag{28}$$

Thus, $\mathbf{T_e}$ and $\dot{\mathbf{T}}_e$ in (27) can be considered as identity matrix and null matrix respectively. Then equation (27) is given by

$$\begin{bmatrix} \dot{x}_A \\ \dot{y}_A \\ \dot{\theta}_A \end{bmatrix} = \begin{bmatrix} -k_1 & 0 & 0 \\ 0 & 0 & v_G \\ 0 & -v_G k_2 & -v_G\left(k_2 k_\theta + \dfrac{1}{k_\theta}\right) \end{bmatrix} \begin{bmatrix} x_A - v_G t \\ y_A \\ \theta_A \end{bmatrix} + \begin{bmatrix} v_G t \\ 0 \\ 0 \end{bmatrix} \tag{29}$$

Equation (29) shows that behavior of x_A is independent from y_A and θ_A. Then, from equation (29), it can be deduced that:

$$\theta_A = \frac{\dot{y}_A}{v_G} \qquad \text{and } \dot{\theta}_A = \frac{\ddot{y}_A}{v_G} \tag{30}$$

From (29) and (30) the following equation can be deduced:

$$\ddot{y}_A + v_G\left(k_2 k_\theta + \frac{1}{k_\theta}\right)\dot{y}_A + v_G^2 k_2 = 0 \tag{31}$$

The damping ratio, ξ determines the characteristics of the system transient response. In the simulations, critical damping was selected. Following similar procedure, the control parameter k_d of the dynamic control part was determined. Fine tuning of the control parameters was done after that to obtain the best system response.

4 SIMULATION AND EXPERIMENTAL RESULTS

For comparison purposes, two controllers have been implemented and simulated in MATLAB: First a kinematic controller that assumes perfect velocity tracking. Second the integrated controller proposed in section 3 which assumes complete knowledge of the mobile robot dynamics including caster wheel effect.

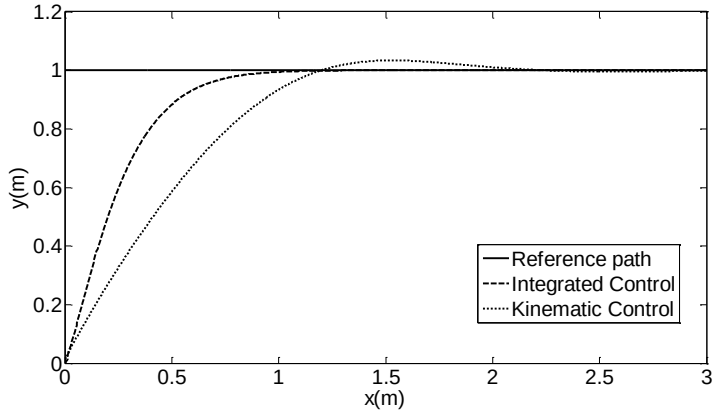

Fig. 5. Comparison Between Kinematic And Integrated Controllers

For a step input reference trajectory, the response of the system using the kinematic and integrated controllers are shown in figure 5. It is clear that the convergence of the robot to the reference path using kinematic controller is slower than that of the integrated one together with the presence of an overshoot. Hence, the performance of the closed loop system using the integrated controller is improved with respect to the kinematic controller.

An experiment for the path following of differential-drive mobile robot using the developed control system has been implemented as shown in figure 6. The mobile robot starts from an initial point on the datum line, and moves until it reaches the step reference path. A chalk is attached to the bottom of the robot to plot the path that the robot follows. Similar to numerical simulations, the robot showed faster convergence and no overshoot when it is controlled by the integrated controller as compared to the kinematic one.

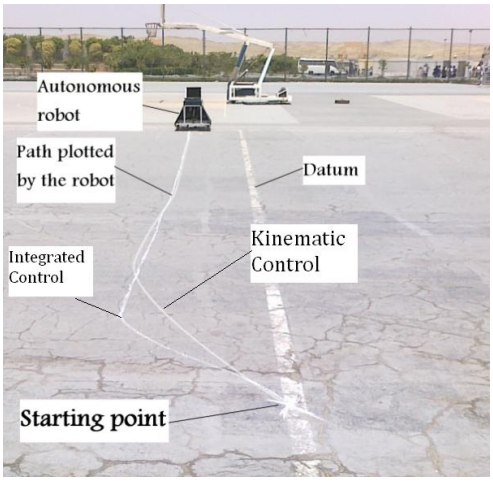

Fig. 6. Path Tracking Experiment

5 CONCLUSIONS

A nonlinear dynamic model of a differential-drive mobile robot including caster-wheel effect has been developed. This model was used in the development of a globally asymptotically stable nonlinear integrated control law for trajectory tracking of nonholonomic mobile robots. The developed controller enhances the performance of controllers commonly used in literature that follows the perfect velocity tracking assumption. Numerical simulations supported by experimental verification show that the developed control law provides faster convergence to the reference path and eliminates overshoot over the kinematic controller alone. The comparison of actual experimental data to the numerical simulations of the analytical model shows the feasibility of the assumptions put forth during the development of the model.

6 REFERENCES

[1] R. Siegwart and R. Nourbakhsh, 2004, *"Introduction to Autonomous Mobile Robots"*, A Bradford Book, The MIT Press, Cambridge, Massachusetts, London, England, 2004.

[2] Y. Kanayama, Y. Kimura, Y., F.Miyazaki, and T. Noguchi, *"A Stable Tracking Control Method for an Autonomous Mobile Rob*ot". Proceeding IEEE International Conference Robotics Automation, 1990, pp. 384–389.

[3] R. Fierro and F. Lewis, "Control of a Nonholonomic Mobile Robot: Backstepping Kinematics into Dynamics", Journal of Robotic Systems, vol. 14, no.3, pp. 149-163, 1997.

[4] Y. Guo, Y. Long and W. Sheng, "*Global Trajectory Generation for Nonholonomic Robots in Dynamic Environments*", IEEE International Conference on Robotics and AutomationRoma, Italy, pp. 10-14 April 2007.
[5] T. Bakker, K. Van Asselt, J. Bontsema, J. Muller and G. Van Straten, "*A Path Following Algorithm For Mobile Robots*", Autonomous Robot, vol. 29: pp. 85–97Springerlink, 2010.
[6] T. H. Lee, H. K. Lam , F. H. F. Leung, P. K. **S.** Tam,"A Fast Path Planning-and-Tracking Control for Wheeled Mobile Robots", proceedings of the 2001 IEEE conference of Robotics & Automation, vol. 1: pp. 1736-1741, 2001.
[7] J. S. Oh, J. B. Park and Y. H. Choi, "*Stable Path Tracking Control of a Mobile Robot Using a Wavelet Based Fuzzy Neural Network*" International Journal of Control, Automation, and Systems, vol. 3, no. 4, pp. 552-563, 2005.
[8] J.L. Martinez, M. Paz and A. García-Cerezo, "*Path Tracking for Mobile Robots with a Trailer.*" 15th Triennial World Congress, Barcelona, Spain, 2002.
[9] C. K. Chen and T. San Dao, "*Dynamics and Path /racking Control of Unmanned Bicycle*", ASME proceedings of IDETC/CIE, 2005.
[10] F. Han, "*Construction of an Omnidirectional Mobile Robot Platform Based on Active Dual-Wheel Caster Mechanisms and Development of a Control Simulator*", Journal of Intelligent and Robotic Systems, vol.9**:** pp. 257–275, 2000.
[11] S. Staicu, "*Dynamics equations of a mobile Robot Provided with Caster Wheel*", Nonlinear Dynamics, vol. 5, pp. 8: 237–248, 2009.

7 Appendix

State-space model (equation 10) coefficients:

$$A_{33} = \frac{-C_l\left\{I_{wr}(l+R)^2+\left(I_R+R^2m_R\right)r_{wr}^{\ 2}\right\}}{r_{wl}^{\ 2}\left(I_{wr}\left(I_R+l^2m_R\right)+I_Rm_Rr_{wr}^{\ 2}\right)+I_{wl}\left(I_{wr}(l+R)^2+\left(I_R+R^2m_R\right)r_{wr}^{\ 2}\right)}$$

$$A_{43} = \frac{-C_l\left(I_R-l_Rm_R\right)r_{wl}r_{wr}}{r_{wl}^{\ 2}\left(I_{wr}\left(I_R+l^2m_R\right)+I_Rm_Rr_{wr}^{\ 2}\right)+I_{wl}\left(I_{wr}(l+R)^2+\left(I_R+R^2m_R\right)r_{wr}^{\ 2}\right)}$$

$$A_{34} = \frac{-C_r\left(I_R-l_Rm_R\right)r_{wl}r_{wr}}{r_{wl}^{\ 2}\left(I_{wr}\left(I_R+l^2m_R\right)+I_Rm_Rr_{wr}^{\ 2}\right)+I_{wl}\left(I_{wr}(l+R)^2+\left(I_R+R^2m_R\right)r_{wr}^{\ 2}\right)}$$

$$A_{44} = \frac{-C_r\left\{I_{wl}(R+l)^2+\left(I_R+l^2m_R\right)r_{wl}^{\ 2}\right\}}{r_{wl}^{\ 2}\left(I_{wr}\left(I_R+l^2m_R\right)+I_Rm_Rr_{wr}^{\ 2}\right)+I_{wl}\left(I_{wr}(l+R)^2+\left(I_R+R^2m_R\right)r_{wr}^{\ 2}\right)}$$

$$B_{31} = \frac{k_{tl}\left\{I_r(l+R)^2+\left(I_R+R^2m_R\right)r_{wr}^{\ 2}\right\}}{r_{wl}^{\ 2}\left(I_{wr}\left(I_R+l^2m_R\right)+I_Rm_Rr_{wr}^{\ 2}\right)+I_{wl}\left(I_{wr}(l+R)^2+\left(I_R+R^2m_R\right)r_{wr}^{\ 2}\right)}$$

$$B_{41} = \frac{k_{tl}\left\{I_R-lRm_R\right\}r_{wl}r_{wr}}{r_{wl}^{\ 2}\left(I_{wr}\left(I_R+l^2m_R\right)+I_Rm_Rr_{wr}^{\ 2}\right)+I_{wl}\left(I_{wr}(l+R)^2+\left(I_R+R^2m_R\right)r_{wr}^{\ 2}\right)}$$

$$B_{32} = \frac{k_{tr}\left\{I_R-lRm_R\right\}r_{wl}r_{wr}}{r_{wl}^{\ 2}\left(I_{wr}\left(I_R+l^2m_R\right)+I_Rm_Rr_{wr}^{\ 2}\right)+I_{wl}\left(I_{wr}(l+R)^2+\left(I_R+R^2m_R\right)r_{wr}^{\ 2}\right)}$$

$$B_{42} = \frac{k_{tr}\left\{I_l(l+R)^2+\left(I_R+l^2m_R\right)r_{wl}^{\ 2}\right\}}{r_{wl}^{\ 2}\left(I_{wr}\left(I_R+l^2m_R\right)+I_Rm_Rr_{wr}^{\ 2}\right)+I_{wl}\left(I_{wr}(l+R)^2+\left(I_R+R^2m_R\right)r_{wr}^{\ 2}\right)}$$

$$B_{33} = \frac{-\left\{r_{wl}\left(I_{wr}(l+R)^2 + \left(I_R + R^2 m_R\right) r_{wr}{}^2\right) N_{wl}\right\}}{r_{wl}{}^2\left(I_{wr}\left(I_R + l^2 m_R\right) + I_R m_R r_{wr}{}^2\right) + I_{wl}\left(I_{wr}(l+R)^2 + \left(I_R + R^2 m_R\right) r_{wr}{}^2\right)}$$

$$B_{43} = \frac{-\left\{\left(I_R - lRm_R\right) r_{wr} r_{wl}{}^2 N_{wl}\right\}}{r_{wl}{}^2\left(I_{wr}\left(I_R + l^2 m_R\right) + I_R m_R r_{wr}{}^2\right) + I_{wl}\left(I_{wr}(l+R)^2 + \left(I_R + R^2 m_R\right) r_{wr}{}^2\right)}$$

$$B_{34} = \frac{-\left\{\left(I_R - lRm_R\right) r_{wl} r_{wr}{}^2 N_{wr}\right\}}{r_{wl}{}^2\left(I_{wr}\left(I_R + l^2 m_R\right) + I_R m_R r_{wr}{}^2\right) + I_{wl}\left(I_{wr}(l+R)^2 + \left(I_R + R^2 m_R\right) r_{wr}{}^2\right)}$$

$$B_{44} = \frac{-\left\{\left(I_l(l+R)^2 + \left(I_R + l^2 m_R\right) r_{wl}{}^2\right)\right\} r_{wr} N_{wr}}{r_{wl}{}^2\left(I_{wr}\left(I_R + l^2 m_R\right) + I_R m_R r_{wr}{}^2\right) + I_{wl}\left(I_{wr}(l+R)^2 + \left(I_R + R^2 m_R\right) r_{wr}{}^2\right)}$$

$$B_{35} = \frac{-r_{wl}\left\{I_{wr}(l+R)(l\sin\beta + L\cos\beta) + \left(I_R \sin\beta + RC_r m_R \cos\beta\right) r_{wr}{}^2\right\}}{r_{wl}{}^2\left(I_{wr}\left(I_R + l^2 m_R\right) + I_R m_R r_{wr}{}^2\right) + I_{wl}\left(I_{wr}(l+R)^2 + \left(I_R + R^2 m_R\right) r_{wr}{}^2\right)}$$

$$B_{45} = \frac{-\left\{I_l(l+R)(R\sin\beta - L\cos\beta) + \left(I_R \sin\beta - lC_r m_R \cos\beta\right) r_{wl}{}^2\right\} r_{wr}}{r_{wl}{}^2\left(I_{wr}\left(I_R + l^2 m_R\right) + I_R m_R r_{wr}{}^2\right) + I_{wl}\left(I_{wr}(l+R)^2 + \left(I_R + R^2 m_R\right) r_{wr}{}^2\right)}$$

$$B_{36} = \frac{r_{wl}\left\{I_r(l+R)(l\cos\beta - L\sin\beta) + \left(I_R \cos\beta - RC_r m_R \sin\beta\right) r_{wr}{}^2\right\}}{r_{wl}{}^2\left(I_{wr}\left(I_R + l^2 m_R\right) + I_R m_R r_{wr}{}^2\right) + I_{wl}\left(I_{wr}(l+R)^2 + \left(I_R + R^2 m_R\right) r_{wr}{}^2\right)}$$

$$B_{46} = \frac{-\left\{\left(I_r(l+R)(R\cos\beta + L\sin\beta) + \left(I_R \cos\beta + m_R C_r l \sin\beta\right) r_{wr}{}^2\right) r_{wr}\right\}}{r_{wl}{}^2\left(I_{wr}\left(I_R + l^2 m_R\right) + I_R m_R r_{wr}{}^2\right) + I_{wl}\left(I_{wr}(l+R)^2 + \left(I_R + R^2 m_R\right) r_{wr}{}^2\right)}$$